Journal of Chemistry and Technologies, 2025, *33*(4), 1010-1017

Journal of Chemistry and Technologies

pISSN 2663-2934 (Print), ISSN 2663-2942 (Online).

journal homepage: http://chemistry.dnu.dp.ua
editorial e-mail: chem.dnu@gmail.com

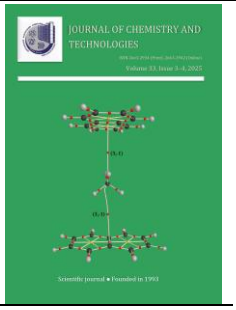

UDC 546(722, 811, 86, 22)

NEW QUATERNARY COMPOUND $FeGdSbS_4$ IN THE $FeSb_2S_4$–$FeGd_2S_4$ SYSTEM

Gulnara N. Ismayilova[1], Sharafat H. Mammadov[2]

[1]*Azerbaijan State Pedagogical University*

[2]*Institute of Catalysis and Inorganic Chemistry named after academician M.F. Nagiev, Azerbaijan, AZ 1143, Baku, G. Javid Ave. 113*

Received 3 June 2025; accepted 18 September 2025; available online 25 December 2025

Abstract

For the first time, the quaternary compound $FeGdSbS_4$ was studied using various physicochemical methods over a wide temperature range. The study of the $FeSb_2S_4$–$FeGd_2S_4$ system revealed that at a ratio of $FeSb_2S_4$:$FeGd_2S_4$ = 1:1, the quaternary compound $FeGdSbS_4$ forms. $FeGdSbS_4$ melts congruently at 1200 K and has a berthierite-type structure (a = 11.382, b = 13.896, c = 3.614 Å; Z = 4; V = 571.606 Å^3, space group Pbam). The specific electrical conductivity of $FeGdSbS_4$ at room temperature is 2×10^{-4} Om^{-1}·m^{-1}. $FeGdSbS_4$ is an impurity semiconductor. The thermal band gap ΔEg of $FeGdSbS_4$ is 1.31 eV. Investigation of the magnitude and sign of the thermoelectric power (TEP) and thermal conductivity in the $FeSb_2S_4$–$FeGd_2S_4$ system shows that both dependencies reach their maxima at the composition corresponding to $FeGdSbS_4$. The Seebeck coefficient (α) for $FeGdSbS_4$ is 1000 mkV/K, and the thermal conductivity is 1.32 Vt/m·K. The $FeSb_2S_4$–$FeGd_2S_4$ system is a quasi-binary section characterized by the formation of a quaternary compound $FeGdSbS_4$, which melts congruently and belongs to the berthierite structural type.

Keywords: quaternary compound; crystal structure; congruent melting; berthierite; thermal effects.

НОВА ЧЕТВЕРНА СПОЛУКА $FeGdSbS_4$ У СИСТЕМІ $FeSb_2S_4$–$FeGd_2S_4$

Гульнара Н. Ісмаїлова[1], Шарафат Г. Мамедов[2]

[1]*Азербайджанський державний педагогічний університет ім*

[2]*Інститут каталізу та неорганічної хімії імені академіка М.Ф. Нагієв, Азербайджан, AZ 1143, Баку, пр. Г. Джавіда 113*

Анотація

Вперше різними фізико-хімічними методами в широкому інтервалі температур вивчено четверну сполуку $FeGdSbS_4$. Під час дослідження системи $FeSb_2S_4$-$FeGd_2S_4$ виявлено, що за співвідношення $FeSb_2S_4$-$FeGd_2S_4$ = 1 : 1 у ній утворюється четверна сполука $FeGdSbS_4$. Сполука $FeGdSbS_4$ плавиться конгруентно за 1200 К і має структуру бертьєріта (a = 11.382, b = 13.896, c = 3.614 Å; Z = 4; V = 571.606 Å^3, просторова група *Pbam*). Питома електропровідність сполуки $FeGdSbS_4$ за кімнатної температури дорівнює $2\cdot10^{-4}$ Ом$^{-1}$·м$^{-1}$. Четверна сполука $FeGdSbS_4$ є домішковим напівпровідником. Термічна ширина забороненої зони Eg для $FeGdSbS_4$ дорівнює 1.31 еВ. Дослідження величини та знака термо-ЕРС у системі $FeSb_2S_4$-$FeGd_2S_4$ та теплопровідності показують, що обидві залежності мають максимуми на складі сполуки $FeGdSbS_4$. Коефіцієнт термо-ЕРС (α) для $FeGdSbS_4$ дорівнює 1000 мкВ/К, а коефіцієнт теплопровідності дорівнює 1.32 Вт/м·град відповідно. Система $FeSb_2S_4$-$FeGd_2S_4$ є квазібінарним перетином і характеризується утворенням четверної сполуки $FeGdSbS_4$, яка плавиться конгруентно і належить до структурного типу бертьєриту.

Ключові слова: четверна сполука; кристалічна структура; плавиться конгруентно; бертьєріт; термічні ефекти.

**Corresponding author: email: chemminfo@gmail.com*

doi: 10.15421/jchemtech.v33i4.331664

Journal of Chemistry and Technologies, 2025, *33*(4), 1010-1017

Introduction

In recent years, there has been a growing interest in ternary and quaternary compounds involving rareearth elements, as well as iron, lead, antimony, and bismuth, which exhibit a wide range of physical properties [1–11]. Due to their valuable physical characteristics, they have become promising objects of study in modern materials science.

It is known that obtaining crystals with properties of practical importance remains one of the major challenges of contemporary science and is a crucial factor in scientific and technological progress. The production of synthetic crystals largely determines the advancement of such important technical fields as radioelectronics, semiconductor and quantum electronics, optical technology, acoustics, and others.

Targeted synthesis, structural pattern identification, and establishing correlations between structure and formation conditions of new phases on one hand, and between physicochemical properties and structure on the other, are essential for synthesizing materials with desired properties.

Due to the known crystal-chemical similarities among lead, antimony, bismuth, and rare-earth elements, synthesizing compounds with these elements and stable cationic or anionic groups is necessary to explore their influence on phase formation and physical properties. Therefore, the synthesis, study of crystal-chemical features, and determination of physicochemical and electrophysical properties of newly formed quaternary phases are highly relevant. They hold both applied value (development of new materials, improvement of synthesis technologies, and crystal growth) and theoretical significance as a foundation for predicting new compounds and their properties.

The search for new functionally promising materials, especially the growth of high-purity single crystals, and the study of the temperature-composition dependencies in related systems are of great technological importance [12–16].

Berthierite ($FeSb_2S_4$) compounds belonging to the family of ternary and quaternary chalcogenides possess a unique set of physical properties. Based on single crystals of these compounds, laboratory laser and acousto-optic devices, high-speed selective radiation receivers for near and mid-IR spectral regions, laser radiation control devices, wide-aperture optical shutters, and contactless temperature measuring instruments have been developed. Considering the above, obtaining quaternary phases based on the indicated minerals by substituting Sb atoms with corresponding rare earth atoms is relevant. On the other hand, currently for nonlinear optics purposes, particularly for controlling powerful laser radiation in the infrared spectral region, there is a need to grow single crystals of quaternary compounds with "large" dimensions and high perfection. Information about defect presence and distribution is essential for developing reproducible crystal growth technologies. Studying the real structure and its defects allows for optimization of synthetic crystal growth through various control techniques. This approach was used to determine the optimal technological parameters for producing large, high-quality single crystals of berthierite-derived compounds.

The Fe–Sb–S system is characterized by various sulfide compounds known in geology and mineralogy. Many of the complex sulfides formed in this system not only possess stable crystalline structures but also exhibit interesting electrical conductivity and magnetic behavior. In particular, several studies have reported on the thermoelectric properties of Fe-based antimonides, highlighting their potential for promising energy applications [17–26]

On the other hand, information on the Fe–Gd–S system in the open literature is very limited. Nevertheless, sulfides enriched with rare-earth elements are known to possess distinctive magnetic and electronic properties. The strong magnetic moment of gadolinium (Gd) ions makes such systems especially interesting for studying additional magnetism and spin–lattice interactions. Therefore, the investigation of new Fe–Gd–S-based compounds is of significant importance from both fundamental and applied perspectives.

It should be noted that there is insufficient information in open sources regarding the physical and structural properties of $FeSb_2S_4$ and $FeGd_2S_4$ compounds. This lack of data indicates that their study not only fills a gap in the existing literature but also provides additional scientific insights into the formation features of the novel quaternary Fe–Sb–Gd–S system. Thus, research in this direction contributes both to the understanding of the fundamental properties of the materials and to the identification of their potential future applications.

Journal of Chemistry and Technologies, 2025, *33*(4), 1010-1017

Experimental part

Due to the absence of information on the phase diagram of the $FeSb_2S_4$–$FeGd_2S_4$ system in the literature, the interaction between the initial ternary sulfides was investigated to determine the possibility of forming a quaternary compound derived from berthierite ($FeSb_2S_4$).

The sSamples were synthesized from ligatures in evacuated quartz ampoules at 1270–1320 K for 24–48 hours. To achieve equilibrium, the alloys were annealed for 700 hours at 900 K. Compositions, thermal effects, and selected physicochemical data of the alloys are provided in Table 1.

Compounds of the $FeGdSbS_4$ type are stable in air and insoluble in alkalis, water, and organic solvents.

The resulting compound was studied by the following methods: differential thermal analysis (DTA), X-ray phase analysis (XRD), microstructural analysis (MSA), and density measurement. XRD was carried out using a D2 PHASER diffractometer with CuKα radiation (Ni filter). DTA was performed in evacuated quartz ampoules using a NETZSCH 404 F1 Pegasus system with NETZSCH Proteus software. The temperature measurement accuracy was ±2 K. MSA was conducted with a MIM-7 microscope. Microhardness was measured using a PMT-3 device. The density was determined by the pycnometric method (toluene was used as a filler).

Alloys with higher $FeGd_2S_4$ content appear dark gray, while those richer in iron thioantimonite (berthierite) appear gray with a metallic luster. The $FeSb_2S_4$–$FeGd_2S_4$ system was studied over the entire concentration range. All thermal effects in the thermograms are endothermic and reversible. As shown in Table 1, two thermal effects related to the liquidus and solidus are observed on the thermograms, except for the 1 : 1 alloy composition, which exhibits a single endothermic effect at 1200 K.

Table 1

Results of DTA, MSA and microhardness measurements of alloys of the $FeSb_2S_4$-$FeGd_2S_4$ system

Composition, mol.%		Thermal effects of heating, K	Density, g/cm³	Microhardness, kg/mm²	Phase composition
$FeSb_2S_4$	$FeGd_2S_4$				
100	0,0	1030	4,65	145	α($FeSb_2S_4$)
95	5,0	995,1050	4,63	170	α
90	10	1000, 1070	4,60	170	α
85	15	1000, 1090	4,76	170	α
80	20	1010, 1120	4,80	185	α
75	25	1025, 1130	-	190	α
70	30	1045, 1160	4,90	190	α
65	35	1060, 1170	-	200	α
60	40	1090, 1175	4,95	215	α
55	45	1050, 1190	-	220	α
50	50	1200	5,12	220	$FeGdSbS_4$
45	55	1000,1170	5,18	220	α + $FeGd_2S_4$
40	60	1000,1130	-	220	α + $FeGd_2S_4$
35	65	1000,1075	5,24	220	α + $FeGd_2S_4$
30	70	1000	5,27	eutectic	α + $FeGd_2S_4$
25	75	1000,1170	5,34	248	α + $FeGd_2S_4$
20	80	1000,1300	5,38	248	α + $FeGd_2S_4$
15	85	1000,1400	5,40	245	α + $FeGd_2S_4$
10	90	1000	5,42	248	α + $FeGd_2S_4$
0,0	100	1620	5,44	248	$FeGd_2S_4$

Results and discussion

Based on the data of physical and chemical analysis and electrophysical measurements, a phase diagram of the $FeSb_2S_4$-$FeGd_2S_4$ system was constructed, shown in Fig. 1. As can be seen from the phase diagram, a complex chemical interaction occurs in the system with the formation of a quaternary compound and a wide range of solid solutions based on betherite.

Journal of Chemistry and Technologies, 2025, *33*(4), 1010-1017

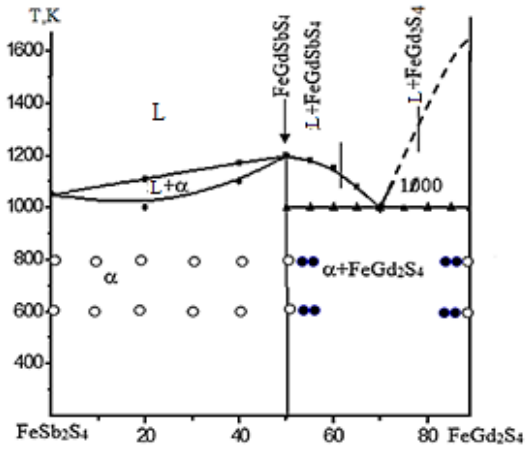

Fig. 1. Phase diagram of the $FeSb_2S_4$-$FeGd_2S_4$ system ○ – single-phase alloys; ● – two-phase alloys

The phase diagram can be represented as two subsystems: $FeSb_2S_4$-$FeGdSbS_4$ and $FeGdSbS_4$-$FeGd_2S_4$. In the $FeSb_2S_4$-$FeGdSbS_4$ subsystem, a single-phase region was found in the concentration range of 0-50 mol% $FeGd_2S_4$. The composition of the compound on which this region of homogeneity is based probably corresponds to the formula $FeSb_{2-x}Gd_xS_4$ (x = 0–1.0) and represents a phase of variable composition. The compound $FeGdSbS_4$ melts congruently at 1200 K and has a berthierite structure (a = 11.382, b = 13.896, c = 3.614 Å; Z = 4; V = 571.606 Å^3, simple group *Pbam*). The formation of a new phase in the $FeSb_2S_4$-$FeGd_2S_4$ system is also confirmed by XRD data (Table.2.)

Table 2

hkl indices, interplanar distances, and intensities of the $FeCdSbS_4$ compound

h	*k*	*l*	*d (Å)*	*I*
1	1	0	8.8053	100
1	2	0	5.9304	44
2	1	0	5.2665	34
0	2	0	6.9480	31
1	1	1	3.3433	25
2	2	0	4.4026	23
1	3	0	4.2903	22
1	2	1	3.0861	21
2	0	0	5.6910	20
2	1	1	2.9799	19
2	2	1	2.7934	16
1	3	1	2.7640	16
3	1	0	3.6600	15
2	3	0	3.5925	15
3	1	1	2.5716	13
2	3	1	2.5478	13
3	2	0	3.3299	12
1	4	0	3.3227	12
3	2	1	2.4489	12
1	4	1	2.4460	12
0	2	1	3.2062	11
2	0	1	3.0508	10
2	4	1	2.2924	10
3	3	1	2.2784	10
2	4	0	2.9652	9
3	3	0	2.9351	9
4	1	1	2.2073	9
1	5	1	2.1630	8
4	1	0	2.7877	8
4	2	1	2.1282	8
3	4	1	2.0902	8
0	0	1	3.6140	7

Journal of Chemistry and Technologies, 2025, *33*(4), 1010-1017

The alloy quenched at 800 K and containing 55 mol.% $FeGd_2S_4$ is two-phase and contains a small amount of the compound $FeGd_2S_4$. The eutectic endoeffect is clearly visible in the thermograms of samples with 55–90 mol.% $FeGd_2S_4$. The eutectic cone (1000 K) in the particular $FeGdSbS_4$-$FeGd_2S_4$ system extends to the ordinate of the $FeGdSbS_4$ compound. The invariant eutectic point corresponds to a concentration of 30 mol.% $FeSb_2S_4$. Temperatures above 1400 K are not shown on the liquidus curve (Fig. 1), since the measurement error value in this temperature region increases significantly.

The particular subsystem $FeSb_2S_4$-$FeGdSbS_4$ is characterized by the formation of a region of solid solutions of the berthierite type. The crystal lattice parameters of solid solutions in the concentration range 0-50 mol.% $FeSb_2S_4$ change as follows: a=11.44–11.382, b=14.12–13.896, c=3.76–3.614 Å (Fig. 2.).

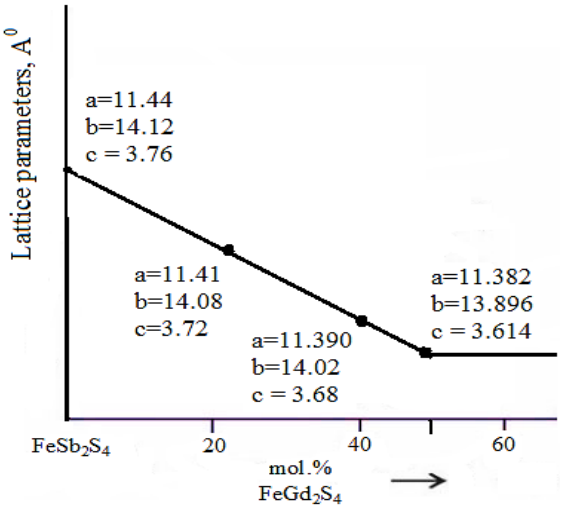

Fig. 2. Lattice parameters of solid solutions of the $FeSb_2S_4$–$FeGd_2S_4$ system

The boundaries of the solid solution region were determined using quantitative phase analysis of alloys annealed at 800 and 600 K and quenched from these temperatures. All lines in the $FeGdSbS_4$ X-ray diffraction pattern are satisfactorily indicated in the rhombic lattice with parameters a=11.382, b=13.896, c=3.614 Å and belong to the berthierite $FeSb_2S_4$ structural type.

The results of the microstructural analysis show that in the $FeSb_2S_4$–$FeCd_2S_4$ section, a solid solution region containing 50 mol% $FeCd_2S_4$ formed on the basis of $FeSb_2S_4$ is present. The formation of this region confirms the tendency toward stable solid solution formation in the system. Furthermore, during the investigation, characteristic microstructural images of the $FeCdSbS_4$ compound were obtained, which clearly demonstrate the effect of compositional variations at the microstructural level (Fig.3).

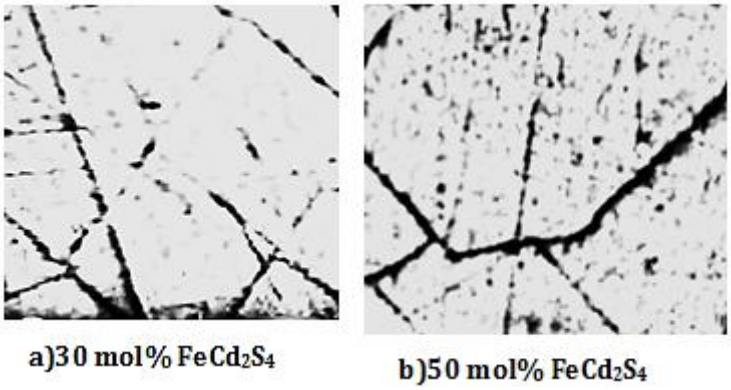

Fig. 3. Microstructures of $FeSb_2S_4$-based samples

Journal of Chemistry and Technologies, 2025, *33*(4), 1010-1017

As can be seen from the figure, the solid solution region of the $FeSb_2S_4$–$FeGd_2S_4$ system (30 mol% $FeGd_2S_4$) has a predominantly homogeneous microstructure with no evidence of secondary phase separation. The visible dark lines correspond to cracks formed as a result of cooling stresses.

$FeCdSbS_4$ compound (50 mol% $FeCd_2S_4$) has a generally homogeneous structure. The dark lines observed within the matrix mainly correspond to cracks formed under the influence of internal stresses; no secondary phase separation is observed.

The formation of a new phase in the $FeSb_2S_4$-$FeGd_2S_4$ system is also confirmed by measuring the electrophysical parameters of the alloys depending on the composition. Fig. 4 shows the concentration dependence of the specific electrical conductivity of the $FeGd_2S_4$-$FeSb_2S_4$ system alloys at room temperature.

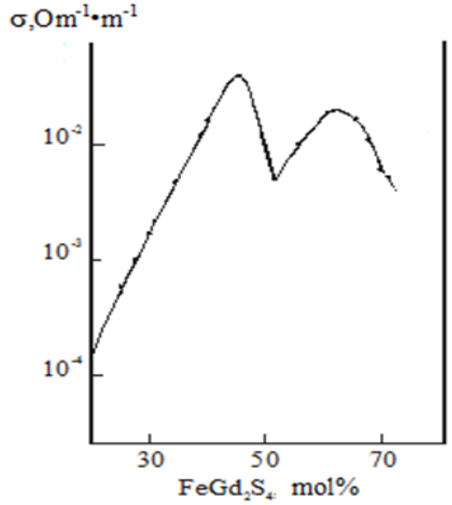

Fig. 4. Concentration dependence of the coefficient of specific electrical conductivity (σ) of alloys in the $FeSb_2S_4$-$FeGd_2S_4$ system

The curve $\sigma = f(x)$ has a clearly defined minimum at the composition of 50 mol% $FeGd_2S_4$, which confirms the existence of the compound $FeGdSbS_4$. The specific electrical conductivity of the compound $FeGdSbS_4$ at room temperature is $2 \cdot 10^{-4}$ $Om^{-1} \cdot m^{-1}$. The quaternary compound $FeGdSbS_4$ is an impurity semiconductor.

The thermal band gap ΔEg of $FeGdSbS_4$ is 1.31 eV. The depth of impurity levels is 0.5 eV.

A study of the magnitude and value of the thermo-emf in the $FeSb_2S_4$-$FeGd_2S_4$ system (Fig. 5) and thermal conductivity (Fig.6) shows that both dependences have maxima on the composition of the $FeGdSbS_4$ compound.

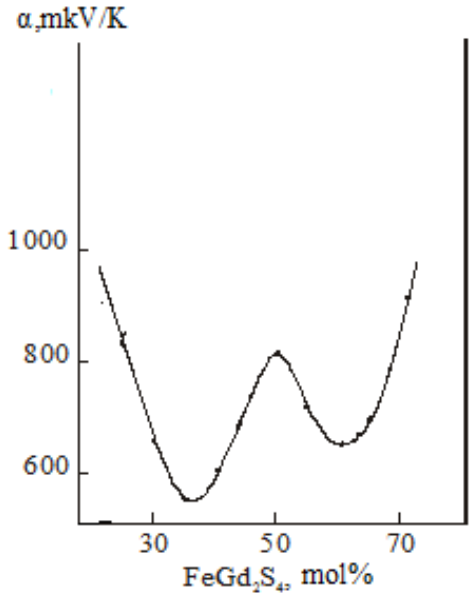

Fig. 5. Concentration dependence of the thermo-emf coefficient (α) of alloys in the $FeSb_2S_4$-$FeGd_2S_4$ system

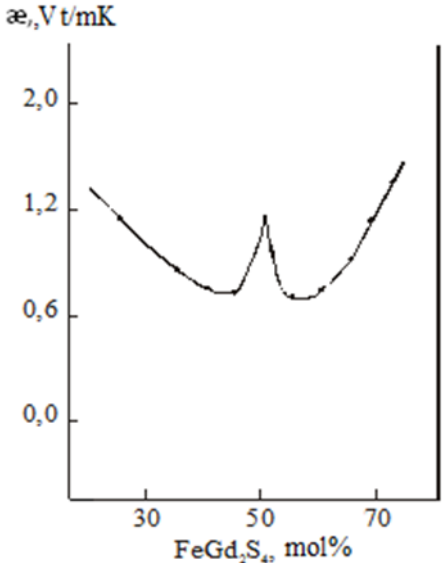

Fig. 6. Concentration dependence of the thermal conductivity coefficient (æ) of alloys in the $FeSb_2S_4$-$FeGd_2S_4$ system

The thermoelectric power coefficients (α) for $FeGdSbS_4$ are 1000 mkV/K, and the thermal conductivity coefficient is 1.32 Vt/mK, respectively.

According to X-ray phase analysis data, in alloys containing 0–50 mol.% $FeGd_2S_4$, only $FeSb_2S_4$ diffraction lines are involved, and in the concentration range of 50–100 mol.% $FeGd_2S_4$, α-solid solutions based on $FeGdSbS_4$ and ternary sulfide $FeGd_2S_4$ crystallize together.

Thus, the $FeSb_2S_4$-$FeGd_2S_4$ system is a quasi-binary section and the formation character of the quaternary compound $FeGdSbS_4$ is smoothly congruent and associated with the berthierite structural type.

Conclusion

1. The quaternary compound $FeGdSbS_4$ was studied using physicochemical methods over a wide temperature range. It melts congruently at 1200 K and has a berthierite structure (a = 11.382, b = 13.896, c = 3.614 Å; Z = 4; V = 571.606 $Å^3$; space group *Pbam*).
2. The quaternary compound $FeGdSbS_4$ is an impurity semiconductor.
3. 3.The specific electrical conductivity at room temperature is $2 \cdot 10^{-4}$ $Om^{-1} \cdot m^{-1}$.
4. The thermal band gap ΔEg of $FeGdSbS_4$ is 1.31 eV

Conflict of interest

The authors declare no conflict of interest.

References

[1] Peng, Q., Hu, X., Zeng, T., Shang, B., Mao, M., Jiao, X., Xi, G. (2020). $FeSb_2S_4$ anchored on amine-modified graphene towards high-performance anode material for sodium ion batteries. *Chemical engineering journal*, *385*, 123857–123865. https://10.1016/j.cej.2019.123857

[2] Wang, P., Ding, Y., Chu, Y., Zhu, X., Lin, J., Shao, L., Zeng, T. (2023). Nano $FeSb_2S_4$ Anchored on Exfoliated Graphite for Sodium-Ion Battery Anode via a Two-Step Fabrication. *American Chemical Society*, 5577–5585. https://10.1021/acs.energyfuels.3c00106

[3] Wintenberger, M., André, G. (1990). Magnetic properties and spiral magnetic structure of berthierite $FeSb_2S_4$. *Physica. B, Condensed matter*, *162*(1), 5–12. https://10.1016/0921-4526(90)90086-A

[4] Wintenberger, M., André, G. (1989). Magnetic structure of the mineral berthierite $FeSb_2S_4$. *Physica. B, Condensed matter*, 156–157, https://10.1016/0921-4526(89)90664-9

[5] Liu, Y., Kang, C.-J., Stavitski, E., Du, Q., Petrovic, C. (2018). Polaronic transport and thermoelectricity in Fe_1-x$Co_x$$Sb_2S_4$ (x=0,0.1,0.2), *Phys. Rev. B, 97*, 155202

[6] Anwar, A., Noor, N. A., Mustafa, G. M., Atiq, S., Ibrahim, A. Laref, A. (2025). Mechanically robust and thermodynamically stable $FeSc_2Z_4$ (Z = S, Se) spinels for future spintronic architectures, *RSC Advances,* 15 (43), 35770–35781. doi: 10.1039/D5RA04959H.

[7] Furqan, M., Mustafa, G. M., Dawas Alkhaldi, H., Alhajri, F., Ameereh, G. I., Al Anazy, M. M., El Rayyes, A. Mahmood, Q. (2025). Study of the electronic, magnetic, and thermoelectric aspects of spinel chalcogenides $SrCe_2Z_4$ (Z = Te, Se, S) for spintronic and energy applications, *RSC Advances, 15*(44), 37288–37298 doi: 10.1039/D5RA03092G.

[8] Noor, N. A., Tahir, M., Khan, M. A., Niaz, S., Ullah, H., Neffati, R. Sharma, R. (2023). Theoretical study of rare

earth in spinel chalcogenide $MgCe_2Z_4$ (Z = S, Se) for spintronic and thermo electric applications, *Materials Science in Semiconductor Processing, 163*, 107563. doi: 10.1016/j.mssp.2023.107563.

[9] Rouf, S.A., Albalawi, H., Zelai, T., Hakami, O., Kattan, N.A. Al Qaisi, S., Younas, M., Hussein, K. I., Mahmood, Q. (2023). Half metallic ferromagnetism and thermoelectric effect in spinel chalcogenides SrX_2S_4 (X = Mn, Fe, Co) for spintronics and energy harvesting, *Journal of Physics and Chemistry of Solids, 182*, 111601. doi: 10.1016/j.jpcs.2023.111601.

[10] Zhang, L., Qin, B., Sun, C., Ji, Y. Zhao, D. (2023). Effect of synthesis factors on microstructure and thermoelectric properties of $FeTe_2$, *Materials, 16*(22), 7170 doi: 10.3390/1996 1944/16/22/7170.

[11] Ramzan, A., Sofi, M. Y., ul Islam, M. I., Khan, M. Sh., Khan, M. A. (2025). Half metallic ferromagnetism and thermoelectric efficient behavior in chalcogenide spinels $MgNi_2X_4$ (X = S, Se): a first principles approach, *RSC Advances, 15*(29), 24002–24018. doi: 10.1039/D5RA03555D

[12] Mammadov, Sh. H., Gurbanov G.R., Ismailova R. A. (2025). Phase diagram of the AgGaS2–PbGa2S4 system. *Voprosy Khimii i Khimicheskoi Tekhnologii,* (1), 22–26. https://doi:10.32434/0321-4095-2025-158-1-22-26

[13] Mammadov, Sh.H., Mammadov A.N., Kurbanova R.C. (2020). Quasi-Binary Section Ag_2SnS_3–$AgSbS_2$. *Russian Journal of Inorganic Chemistry*, *65*(2), 217–221. https://doi.org/10.1134/S003602362001012X

[14] Mammadov, F.M. (2020). FeS-FeGa2S4-FeGaInS4 system. *Chemical Problems*, *18*(2), 214–221. https://doi.org/10.32737/2221-8688-2020-2-214-221

[15] Mammadov, F. M. (2021). New version of the phase diagram of the MnTe-Ga_2Te_3 system. *New Materials, Compounds and Applications, 5*(2), 116–121.

[16] Mammadov, Sh.H. (2020). The study of the quasi-triple system FeS-Ga_2S_3-Ag_2S by a $FeGa_2S_4$-$AgGaS_2$ section. *Kondensirovannye Sredy Mezhfaznye Granitsy*, *22*(2), 232–237. https://doi.org/10.17308/kcmf.2020.22/2835

[17] Dixit, A., Ahmed, I., Abraham, J., El‐Bahy, Z. M. (2024). Optoelectronic and thermoelectric properties of spinel chalcogenides $HgLa_2X_4$ (X = S, Se): A first‐principles study, *Journal of Rare Earths, 42*(10), 1927–1936. doi: 10.1016/j.jre.2023.11.014.

[18] Suraj, K. S., Eivari, H. A., Tatara, G. Assadi, M. H. N. (2024). Tripling magnetite's thermoelectric figure of merit with rare earth doping, *Journal of Materials Chemistry C, 12*(36), 19212–19218. doi: 10.1039/D4TC03153A.

[19] Zeng, Q., Sameeullah, M., Ali, H. (2025). DFT study of chalcogenide spinels $MnSc_2X_4$ (X = S, Se): structural, electronic and thermoelectric behaviour, *RSC Advances, 15*(22), 9662–9675. doi: 10.1039/D4RA08334B.

[20] Nazir, G., Alofi, A. S., Rehman, A., Mahmood, Q., Al‐Anazy, M. Rahman, M. F. (2024). Rare earth based Mg‐chalcogenides $MgDy_2(S/Se)_4$ as an emerging aspirant for spintronic and thermoelectric applications, *Materials Science in Semiconductor Processing*, *173*, 108129. doi: 10.1016/j.mssp.2024.108129

[21] Koc, A., Akbulut, H., Senol, S. (2024). Investigation of structural, optical, and thermoelectric properties of $ZnFe_2O_4$ and Ni‐doped $ZnFe_2O_4$, *Ceramics International*, *50*(22), 45251–45262. doi: 10.1016/j.ceramint.2024.08.365.

[22] Li, J., Xie, Y., Wang, Q., Zhao, X. (2023). Magnetic and thermoelectric properties of rare‐earth substituted spinel ferrites: A review, *Journal of Magnetism and Magnetic Materials*, *543*, 168780

[23] Wei, Z., Deng, Y., Peng, P., Zhang, Y. Zheng, Z. (2025). Advances in silver‐based chalcogenide flexible thermoelectric materials, *CrystEngComm, 27*(8), 1055–1077 doi: 10.1039/D4CE00915K.

[24] Kabir, S. M., Rahman, M. T., Hossain, M. Z. R. (2024). ecent progress in chalcogenide spinels for thermoelectric applications, *Journal of Materials Science: Materials in Electronics, 35*, 4021–4045

[25] Patel, R., Singh, D., Kumar, V. (2024). Density functional study of structural and thermoelectric properties of chalcogenide AB_2X_4 compounds, *Computational Materials Science,* 221, 112552

[26] Gao, L., Zhou, H., Chen, G. (2025). Spinel chalcogenides as multifunctional materials for energy harvesting: synthesis and properties, *Progress in Materials Science*, *139*, 101148.